REVISTA MEXICANA DE FÍSICA S **54** (3) 122–128 DICIEMBRE 2008

Projected shell model description for nuclear isomers

Yang Sun
Department of Physics, Shanghai Jiao Tong University,
Shanghai 200240, P.R. China,
Joint Institute for Nuclear Astrophysics, University of Notre Dame,
Notre Dame, Indiana 46545, USA.

Recibido el 10 de marzo de 2008; aceptado el 7 de mayo de 2008

The study of nuclear isomer properties is a current research focus. To describe isomers, we present a method based on the Projected Shell Model. Two kinds of isomers, K-isomers and shape isomers, are discussed. For the K-isomer treatment, K-mixing is properly implemented in the model. It is found however that in order to describe the strong K-violation more efficiently, it may be necessary to further introduce triaxiality into the shell model basis. To treat shape isomers, a scheme is outlined which allows mixing those configurations belonging to different shapes.

Keywords: Shell model; nuclear energy levels.

Se estudian las propiedades de isómeros nucleares a través del modelo de capas proyectadas. Se discutan isómeros K y de forma nuclear. Para discutir las propiedades de los isómeros K se tiene que incluir la mezcla de diferentes valores K en el modelo así como la deformación triaxial. A los isómeros de forma se pueden tratar en un modelo que permita la mezcla de configuraciones con formas nucleares distintas.

Descriptores: Modelo de capas; niveles de energía nucleares.

PACS: 21.60.Cs; 21.10.-k

1. Introduction

A nuclear isomer is an excited state, in which a combination of nuclear structure effects inhibits its decay and endows the isomeric state with a lifetime that can be much longer than most nuclear states. Known isomers in nuclei span the entire range of lifetimes from 10^{15} years for ^{180m}Ta – longer than the accepted age of the universe – to an informal rule of thumb on the lower side of approximately 1 ns. Nuclear isomers decay predominantly by electromagnetic processes (γ-decay or internal conversion). There are also known instances of the decay being initiated by the strong interaction (α-emission) or the weak interaction (β-decay or electron capture). Decay by proton or neutron emission, or even by nuclear fission, is possible for some isomers (see recent examples [1-3].

Often discussed in the literature are three mechanisms [4] leading to nuclear isomerism, although new types of isomer may be possible in exotic nuclei [5]. It is difficult for an isomeric state to change its shape to match the states to which it is decaying, or to change its spin, or to change its spin orientation relative to an axis of symmetry. These correspond to shape isomers, spin traps, and K-isomers, respectively. In any of these cases, decay to the ground state is strongly hindered, either by an energy barrier or by the selection rules of transition. Therefore, isomer lifetimes can be remarkably long. To mention a few examples, an $I^{\pi}=0^{+}$ excited state in ^{72}Kr has been found as a shape isomer [6], a 12^{+} state in ^{98}Cd has been understood as a spin trap [7], and in ^{178}Hf, there is a famous 16^{+}, 31-year K-isomer [8], which has become a discussion focus because of the proposal of using this isomer as energy storage [9].

Detailed nuclear structure studies are at the heart of understanding the formation of nuclear isomers with applications to many aspects in nuclear physics. The study is particularly interesting and important for unstable nuclei, such as those in neutron-rich, proton-rich, and superheavy mass regions. In a quantum system, the ground state is usually more stable than the excited states. However, the lifetime of ground state of unstable nuclei is short, which makes the laboratory study extremely difficult. In contrast, nuclear isomers in those nuclei may be relatively easy to access experimentally. Furthermore, the physics may be changed due to the existence of isomers in those unstable nuclei. It has been pointed out by Xu *et al.* [10] that in superheavy nuclei, the isomeric states decrease the probability for both fission and α-decay, resulting in enhanced stability for these nuclei. One expects that the isomers in very heavy nuclei could serve as stepping stones toward understanding the single-particle structure beyond the Z=82 and N=126 shell closures, which is the key to locating the anticipated 'island of stability' [11].

Moreover, nuclear isomers may play a significant role in determining the abundances of the elements in the universe [12]. In hot astrophysical environments, an isomeric state can communicate with its ground state through thermal excitations. This could alter significantly the elemental abundances produced in nucleosynthesis. The communication between the ground state of ^{26}Al and the first excited isomeric state in this nucleus has the consequence that the astrophysical half-life for ^{26}Al can be much shorter than the laboratory value [13]. One is just beginning to look at the impact that nuclear isomers have on various other nucleosynthesis processes such as the rapid proton capture process thought to take place on the accretion disks of binary neutron stars.

There are cases in which an isomer of sufficiently long lifetime (probably longer than microseconds) may change the paths of reactions taking place and lead to a different set of elemental abundances [14].

With rapidly growing interest in the isomer study and increasing possibility of experimental access to isomeric states, theoretical effort is much needed. The present paper discusses a Projected Shell Model (PSM) description for nuclear isomers. As isomeric states are a special set of nuclear states, special emphasis is given when these states are treated. In Sec. 2 of the paper, we present a description for K-isomers, in which K-mixing is emphasized. We point out, however, that an extended PSM based on triaxially-deformed basis is required to describe the strong K-violation. In Sec. 3, shape isomer examples are presented and a perspective how configurations with different shapes can be mixed is outlined. Finally, the paper is summarized in Sec. 4.

2. K-mixing in the projected shell model

Many long-lived, highly-excited isomers in deformed nuclei owe their existence to the approximate conservation of the K quantum number. The selection rule for an electromagnetic transition would require that the multipolarity of the decay radiation, λ, be at least as large as the change in the K-value ($\lambda \geq \Delta K$). However, symmetry-breaking processes make possible transitions that violate the K-selection rule. A microscopic description of K-violation is through the so-called K-mixing in the configuration space. A theoretical model that can treat K-mixing has preferably the basis states that are eigenstates of angular momentum I but labeled by K. Diagonalization of two-body interactions mixes these states and the resulting wavefunctions contain the information on the degree of K-mixing. In this kind of approach, the mixing and its consequences are discussed in the laboratory frame rather than in a body-fixed frame in which K is originally defined.

2.1. The model

The projected shell model (PSM) [15,16] seems to fulfill the requirement. It is a shell model that starts from a deformed basis. In the PSM, the shell-model basis is constructed by considering a few quasiparticle (qp) orbitals near the Fermi surfaces and performing angular momentum projection (if necessary, also particle-number projection) on the chosen configurations. With projected multi-qp states as the basis states of the model, the PSM is designed to describe the rotational bands built upon qp excitations.

Suppose that a PSM calculation begins with axially deformed Nilsson single-particle states, with pairing correlations incorporated into these states by a BCS calculation. This defines a set of deformed qp states (with $a^\dagger_\nu$ and $a^\dagger_\pi$ being the creation operator for neutrons and protons, respectively) with respect to the qp vacuum $|0\rangle$. The PSM basis is then constructed in the multi-qp states with the following forms

$$\begin{aligned}
\mathrm{e-e\ nuclei}: &\{|0\rangle, a^\dagger_\nu a^\dagger_\nu|0\rangle, a^\dagger_\pi a^\dagger_\pi|0\rangle, a^\dagger_\nu a^\dagger_\nu a^\dagger_\pi a^\dagger_\pi|0\rangle, \\
&a^\dagger_\nu a^\dagger_\nu a^\dagger_\nu a^\dagger_\nu|0\rangle, a^\dagger_\pi a^\dagger_\pi a^\dagger_\pi a^\dagger_\pi|0\rangle, \ldots\} \\
\mathrm{o-o\ nuclei}: &\{a^\dagger_\nu a^\dagger_\pi|0\rangle, a^\dagger_\nu a^\dagger_\nu a^\dagger_\nu a^\dagger_\pi|0\rangle, a^\dagger_\nu a^\dagger_\pi a^\dagger_\pi a^\dagger_\pi|0\rangle, \\
&a^\dagger_\nu a^\dagger_\nu a^\dagger_\nu a^\dagger_\pi a^\dagger_\pi a^\dagger_\pi|0\rangle, \ldots\} \\
\mathrm{odd-}\nu\ \mathrm{nuclei}: &\{a^\dagger_\nu|0\rangle, a^\dagger_\nu a^\dagger_\nu a^\dagger_\nu|0\rangle, a^\dagger_\nu a^\dagger_\pi a^\dagger_\pi|0\rangle, \\
&a^\dagger_\nu a^\dagger_\nu a^\dagger_\nu a^\dagger_\pi a^\dagger_\pi|0\rangle, \ldots\} \\
\mathrm{odd-}\pi\ \mathrm{nuclei}: &\{a^\dagger_\pi|0\rangle, a^\dagger_\nu a^\dagger_\nu a^\dagger_\pi|0\rangle, a^\dagger_\pi a^\dagger_\pi a^\dagger_\pi|0\rangle, \\
&a^\dagger_\nu a^\dagger_\nu a^\dagger_\pi a^\dagger_\pi a^\dagger_\pi|0\rangle, \ldots\}
\end{aligned}$$

The omitted index for each creation operator contains labels for the Nilsson orbitals. In fact, this is the usual way of building multi-qp states [10,17-19].

The angular-momentum-projected multi-qp states, each being labeled by a K quantum number, are thus the building blocks in the PSM wavefunction, which can be generally written as

$$|\psi^{I,\sigma}_M\rangle = \sum_{\kappa,K\leq I} f^{I,\sigma}_\kappa \hat{P}^I_{MK}|\phi_\kappa\rangle = \sum_\kappa f^{I,\sigma}_\kappa \hat{P}^I_{MK_\kappa}|\phi_\kappa\rangle. \quad (1)$$

The index σ denotes states with the same angular momentum and κ labels the basis states. $\hat{P}^I_{MK}$ is the angular-momentum-projection operator [15] and the coefficients $f^{I,\sigma}_\kappa$ are weights of the basis states. The weights $f^{I,\sigma}_\kappa$ are determined by diagonalization of the Hamiltonian in the projected spaces, which leads to the eigenvalue align (for a given I)

$$\sum_{\kappa'} \left(H_{\kappa\kappa'} - E_\sigma N_{\kappa\kappa'}\right) f^\sigma_{\kappa'} = 0. \quad (2)$$

The Hamiltonian and the norm matrix elements in Eq. (2) are given by

$$H_{\kappa\kappa'} = \langle\phi_\kappa|\hat{H}\hat{P}^I_{K_\kappa K'_{\kappa'}}|\phi_{\kappa'}\rangle, \quad N_{\kappa\kappa'} = \langle\phi_\kappa|\hat{P}^I_{K_\kappa K'_{\kappa'}}|\phi_{\kappa'}\rangle. \quad (3)$$

Angular-momentum-projection on a multi-qp state $|\phi_\kappa\rangle$ with a sequence of I generates a band. One may define the rotational energy of a band (band energy) using the expectation values of the Hamiltonian with respect to the projected $|\phi_\kappa\rangle$

$$E^I_\kappa = \frac{H_{\kappa\kappa}}{N_{\kappa\kappa}} = \frac{\langle\phi_\kappa|\hat{H}\hat{P}^I_{K_\kappa K_\kappa}|\phi_\kappa\rangle}{\langle\phi_\kappa|\hat{P}^I_{K_\kappa K_\kappa}|\phi_\kappa\rangle}. \quad (4)$$

In a usual approximation with independent quasiparticle motion, the energy for a multi-qp state is simply taken as the sum of those of single quasiparticles. This is the dominant term. The present theory modifies this quantity in the following two steps. First, the band energy defined in Eq. (4) introduces the correction brought by angular momentum projection and the two-body interactions, which accounts for the couplings between the rotating body and the quasiparticles in a quantum-mechanical way. Second, the corresponding rotational states (labeled by K) are mixed in the subsequent

procedure of solving the eigenvalue Eq. (2). The energies are thus further modified by configuration mixing.

For deformed states with axial symmetry, each of the basis states in Eq. 1, *i.e.* the projected $|\phi_\kappa\rangle$, is a K-state. For example, an n-qp configuration gives rise to a multiplet of 2^{n-1} states, with the total K expressed by $K{=}|K_1 \pm K_2 \pm \cdots \pm K_n|$, where K_i is for an individual neutron or proton. In this case, shell model diagonalization, *i.e.* solving the eigenvalue Eq. (2), is equivalent to K-mixing. The degree of K-mixing can be read from the resulting wavefunctions.

The above discussion is independent of the choice of the two-body interactions in the Hamiltonian. In practical calculations, the PSM uses the separable forces with pairing plus quadrupole-quadrupole terms (these have been known to be essential in nuclear structure calculations [20]), with inclusion of the quadrupole-pairing term

$$\hat{H}{=}\hat{H}_0{-}\frac{1}{2}\chi\sum_\mu \hat{Q}^\dagger_\mu\hat{Q}_\mu - G_M\hat{P}^\dagger\hat{P} - G_Q\sum_\mu \hat{P}^\dagger_\mu\hat{P}_\mu. \quad (5)$$

The strength of the quadrupole-quadrupole force χ is determined in such a way that it holds a self-consistent relation with the quadrupole deformation ε_2. The monopole-pairing force constants G_M are

$$G_M = \left[G_1 \mp G_2\tfrac{N-Z}{A}\right]\ A^{-1}, \quad (6)$$

with "$-$" for neutrons and "$+$" for protons, which roughly reproduces the observed odd–even mass differences in a given mass region when G_1 and G_2 are properly chosen. Finally, the strength G_Q for quadrupole pairing was simply assumed to be proportional to G_M, with a proportionality constant fixed in a nucleus, choosing from the range 0.14 – 0.18.

2.2. The ^{178}Hf example

The nucleus ^{178}Hf has become a discussion focus because of the possibility to trigger the 2.45MeV, 31-year 16^+-isomer decay. The triggering could be made by applying external electromagnetic radiation which, if successful, will lead to the controlled release of nuclear energy [9]. Information on the detailed structure as well as the transition of this and the surrounding states thus becomes a crucial issue. In the PSM calculation for ^{178}Hf [8], the model basis was built with the deformation parameters $\varepsilon_2{=}0.251$ and $\varepsilon_4{=}0.056$. Fig. 1 shows the calculated energy levels in ^{178}Hf, which are compared with the known data [21]. Satisfactory agreement is achieved for most of the states, except that for the bandhead of the first 8^- band and the 14^- band, the theoretical values are too low.

It was found that the obtained states are generally K-mixed. If the mixing is not strong, one may still talk about the dominant structure of each band by studying the wavefunctions. We found that the 6^+ band has mainly a 2-qp structure $\{\nu[512]5/2^- \oplus \nu[514]7/2^-\}$, the 16^+ band has a 4-qp structure

$$\{\nu[514]7/2^- \oplus \nu[624]9/2^+ \oplus \pi[404]7/2^+ \oplus \pi[514]9/2^-\},$$

the first (lower) 8^- band has a 2-qp structure

$$\{\nu[514]7/2^- \oplus \nu[624]9/2^+\},$$

the second (higher) 8^- band has a 2-qp structure

$$\{\pi[404]7/2^+ \oplus \pi[514]9/2^-\},$$

and the 14^- band has a 4-qp structure

$$\{\nu[512]5/2^- \oplus \nu[514]7/2^- \oplus \pi[404]7/2^+ \oplus \pi[514]9/2^-\}.$$

These states, together with many other states (not shown in Fig. 1) obtained from a single diagonalization, form a complete spectrum including the high-K isomeric states.

TABLE I. Comparison of calculated ^{174}Yb ground band with data. $E(I)$ are in keV and $B(E2, I \to I-2)$ in W.u..

Spin I	$E(I)$, Exp	$E(I)$, PSM	$B(E2)$, Exp	$B(E2)$, PSM
2	76.5	71.1	201(7)	195.18
4	253.1	236.7	280(9)	279.01
6	526.0	496.1	370(50)	307.59
8	889.9	848.0	388(21)	322.31
10	1336	1290.3	325(22)	331.28
12	1861	1820	369(23)	337.13
14	2457	2433	320	340.91

As far as energy levels are concerned, the PSM can give a reasonable description simultaneously for multiple bands. The next question is how electromagnetic transitions are described. The electromagnetic transition between any two of these states can be directly calculated [22] by using the wavefunctions. This is a crucial test for the model wavefunctions.

2.3. The $N = 104$ isotones

There have been detailed experimental studies on the 6^+ isomer in some $N{=}104$ isotones [23-25]. These data show that along the $N{=}104$ isotones, lifetime of the 6^+ isomer can vary very much, differing by several orders of magnitude. Understanding the underlying physics is a challenging problem: what is the microscopic mechanism for such a drastic change in the neighboring isotones? PSM calculations are performed for ^{174}Yb. The deformed basis is constructed with deformation parameters $\varepsilon_2 = 0.275$ and $\varepsilon_4 = 0.042$. In Tables I, II, and III, three groups of results are listed, for the $K{=}0$ ground band (Table I) and $K{=}6$ isomer band (Table II) with in-band transitions, and inter-band transitions (Table III) between the ground band and the $K{=}6$ isomer band. These results suggest that while the energy levels for both ground and isomer

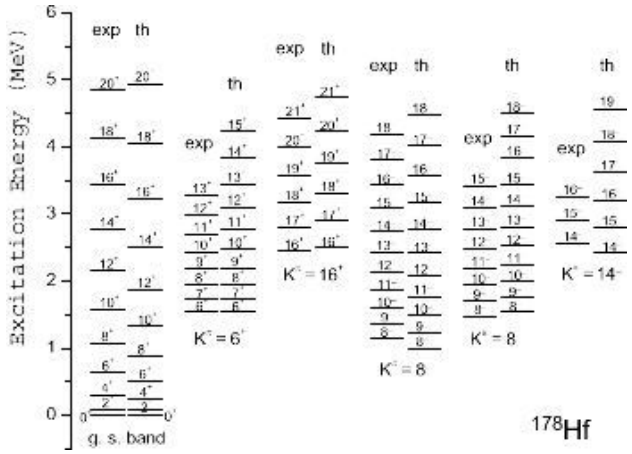

FIGURE 1. Comparison of the PSM calculation with data for the rotational bands in ^{178}Hf . This figure is adopted from Ref. 8

bands are reproduced, the $E(2)$ transition probabilities are also correctly obtained. In particular, the calculation yields a reasonable value of the very small inter-band $B(E2)$ as what was observed in ^{174}Yb [23] (see Table III). Note that without mixing configurations in the wavefunction, a direct transition from the 6^+ isomer to ground band would be forbidden. The obtained amount of inter-band $B(E2)$, though small, is the consequence of K-mixing contained in the PSM.

On the other hand, in its isotones ^{176}Hf and ^{178}W, much enhanced $B(E2)$ from the 6^+ isomer to ground band has been obtained experimentally. The values are 1.8×10^{-5} e^{2}fm^4 for ^{176}Hf and 2.6×10^{-2} e^{2}fm^4 for ^{178}W. If a PSM calculation is performed for these two isotones, one gets similar small numbers for the inter-band $B(E2)$ as in ^{174}Yb, which disagree with data. We have to conclude that although the current PSM has K-mixing mechanism in the model, which effectively introduces γ, the mixing within the truncated space is apparently too weak.

In Fig. 2, we plot experimental excitation energies of the 6^+ isomer states together with 2^+ state of γ vibration for Yb, Hf, and W isotopes. There seems to be an correlation between the two plotted quantities. The correlation is such that to compare with the 2^+ γ states, energy of the 6^+ isomers shows an opposite variation trend with neutron number. At N=104, nuclei have the highest excitation of γ vibrational

TABLE II. Comparison of calculated ^{174}Yb 6^+ isomer band with data. $E(I)$ are in keV and $B(E2, I \to I-2)$ in W.u..

Spin I	$E(I)$, Exp	$E(I)$, PSM	$B(E2)$, PSM
6	1518.0	1503	
7	1671.1	1683	
8	1844.7	1886	36.76
9	2038.3	2117	78.18
10	2251.5	2372	115.81
11	2483.7	2652	147.96
12	2734.4	2956	174.91
13	3003.1	3283	197.41

TABLE III. Comparison of calculated inter-band transition of ^{174}Yb 6^+ isomer to ground band. $B(E2)$ is in e^2fm^4

Transition	$B(E2)$, Exp	$B(E2)$, PSM
$6_i \to 4_g$	$4.3(8) \times 10^{-9}$	8.49×10^{-8}

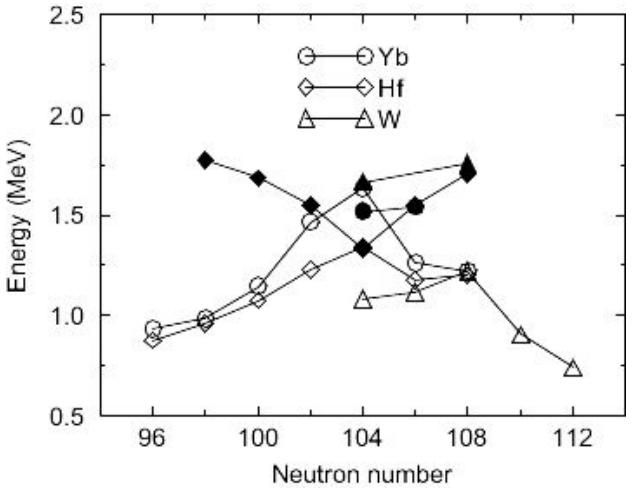

FIGURE 2. Experimental data for excitation energy of I^π=6^+ isomer (filled symbols) and 2^+ γ vibrational state (open symbols).

states while they show a minimum in 6^+ isomer energy. In Fig. 2, ^{174}Yb appears to be the only nucleus in the collection that has the 6^+ isomer lower than the γ states. Therefore, below the 6^+ isomer in ^{174}Yb, there are no γ states carrying finite K to be mixed in the wavefunction. This may have naively explained why the ^{174}Yb isomer decay is so exceptionally hindered.

In Ref. 26, a γ-tunneling model was introduced by Narimatsu, Shimizu, and Shizuma to describe the enhanced $B(E2)$ values. In their model, the γ degree of freedom is taken into account, which breaks the axial symmetry explicitly. The spontaneous symmetry breaking helps in realizing larger electromagnetic transitions which would otherwise be impossible due to the selection rule. In this way, the authors in Ref. 26, were able to describe the observed large inter-band $B(E2)$ in ^{176}Hf and ^{178}W rather successfully. However, their model could not give the above-discussed small $6_i^+ \to 4_g^+$ inter-band $B(E2)$ in ^{174}Yb.

Both methods, the configuration mixing implemented by the PSM and the γ-tunneling by Narimatsu *et al.*, introduce a mechanism to break the axial symmetry; however the degree of symmetry breaking is different. If the physical process is a perturbation in the K space, then it is better described by the PSM based on the axially symmetric mean field. If it is not, axial symmetry in the mean field must be broken as in the γ-tunneling model. The two models may be viewed as two different simplifications of the complicated many-body problem; each emphasizes one aspect. It is desired that one can have one unified microscopic description for all cases.

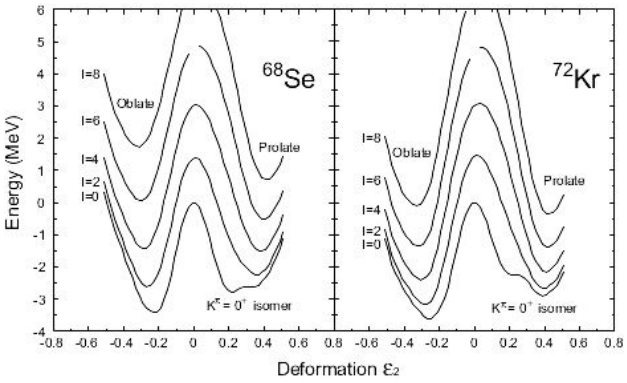

FIGURE 3. Energy surfaces for various spin states in ^{68}Se and ^{72}Kr as functions of deformation variable ε_2. This figure is adopted from Ref. 14.

To efficiently introduce γ degree of freedom within the PSM, one can break the axial symmetry of the single-particle basis and carry out three-dimensional angular momentum projection. The shell model diagonalization is then performed in the projected multi-quasiparticle configurations based on γ deformed basis. One example is the description of γ vibrational states within the PSM. It was shown [27] that by using projected triaxially-deformed basis, it is possible to describe the ground band and γ band simultaneously. Thus, an extended PSM that introduces triaxiality in the model would be useful for cases with large K-violation. Such an extension has recently be developed for odd-odd nuclei [28] and even-even nuclei [29], and will be applied to the isomer study.

3. Shape isomer and configuration mixing

Coexistence of two or more well-developed shapes at comparable excitation energies is a well-known phenomenon. The expected nuclear shapes include, among others, prolate and oblate deformations. In even-even nuclei, an excited 0^+ state may decay to the ground 0^+ state via an electric monopole (E0) transition. For lower excitation energies, the E0 transition is usually very slow, and thus the excited 0^+ state becomes a shape isomer.

3.1. Shape isomer in ^{68}Se and ^{72}Kr and the impact on isotopic abundance in X-ray bursts

Figure 3 shows calculated projected energies as a function of deformation variable ε_2 for different spin states in the $N{=}Z$ nuclei ^{68}Se and ^{72}Kr. The configuration space and the interaction strengths in the Hamiltonian are the same as those employed in the previous calculations for the same mass region [30]. It is found that in both nuclei, the ground state takes an oblate shape with $\varepsilon_2 \approx -0.25$. As spin increases, the oblate minimum moves gradually to $\varepsilon_2 \approx -0.3$. Another local minimum with a prolate shape ($\varepsilon_2 \approx 0.4$) is found to be 1.1 MeV (^{68}Se) and 0.7 MeV (^{72}Kr) high in excitation. Bouchez *et al.* [6] observed the 671 keV shape-isomer in ^{72}Kr with half-life $\tau{=}38 \pm 3$ ns. The one in ^{68}Se is the prediction, awaiting experimental confirmation. Isomers in these nuclei have also been predicted by Kaneko, Hasegawa, and Mizusaki [31].

The existence of low energy 0^+ shape isomer along the $N{=}Z$ nuclei has opened new possibilities for the rp-process [32] reaction path occurring in X-ray burst. Since the ground states of ^{73}Rb and ^{69}Br are bound with respect to these isomers, proton capture on these isomers may lead to additional strong feeding of the ^{73}Rb$(p,\gamma)^{74}$Sr and ^{69}Br$(p,\gamma)^{70}$Kr reactions. However, the lifetime of the isomeric states must be sufficiently long to allow proton capture to take place. No information is available about the lifetime of the ^{68}Se isomer while the 55 ns lifetime of the isomer in ^{72}Kr is reported [6]. Based on Hauser Feshbach estimates [32] the lifetime against proton capture is in the range of $\approx$100 ns to 10 μs depending on the density in the environment. Considering the uncertainties in the present estimates a fair fraction may be leaking out of the ^{68}Se, ^{72}Kr equilibrium abundances towards higher masses.

3.2. Configuration mixing with different shapes

To calculate isomer lifetime, decay probability is needed. This involves transitions from the shape isomer to the ground state, which belong to different shapes or deformation minima. If the energy barrier between the minima is not very high, configuration mixing of the two shapes must be taken into account. In the following, we outline a scheme to consider such a mixing. The discussion is general; the shapes can be any kinds of two deformed ones in a nucleus. For example, one of them can be a prolately-deformed and the other an oblately-deformed shape, or one of them can be a normally-deformed and the other a superdeformed shape. Generalizing the method further, it can describe those transitional nuclei where energy surfaces are typically flat.

The heart of the present consideration is the evaluation of overlapping matrix element in the angular-momentum-projected bases. Let us start with the PSM wave function in Eq. (1).

$$|\psi^{I,\sigma}_M\rangle = \sum_\kappa f^{I,\sigma}_\kappa \hat{P}^I_{MK_\kappa}|\phi_\kappa\rangle.$$

For an overlapping matrix element, states in the left and right hand side must correspond to different deformed shapes. Therefore, two different sets of quasiparticle generated at different deformations are generally involved. Let us denote $|\phi_\kappa\rangle$ explicitly as $|\phi_\kappa(a)\rangle$ and $|\phi_\kappa(b)\rangle$, for which we define two sets of quasiparticle operators $\{a^\dagger\}$ and $\{b^\dagger\}$ associated with the quasiparticle vacua $|a\rangle$ and $|b\rangle$, respectively.

For simplicity, we assume axial symmetry. The general three-dimensional angular momentum projection is reduced to a problem of one-dimensional projection, with the projector having the following form

$$\hat{P}^I_{MK} = \left(I+\frac{1}{2}\right)\int_0^\pi d\beta\ \sin\beta\ d^I_{MK}(\beta)\ \hat{R}_y(\beta) \quad (7)$$

with

$$\hat{R}_y(\beta) = e^{-i\beta\hat{J}_y}. \tag{8}$$

In Eq. (7), $d^I_{MK}(\beta)$ is the small-d function and β is one of the Euler angels. The evaluation of the overlapping matrix element is eventually reduced to the problem

$$\langle\Phi_{\kappa'}(b)|\,\hat{O}\hat{R}_y(\beta)\,|\Phi_\kappa(a)\rangle\,, \tag{9}$$

which is the problem of calculating the $\hat{O}$ operator sandwiched by a multi-qp state $|\Phi_{\kappa'}(b)\rangle$ and a *rotated* multi-qp state $\hat{R}_y(\beta)\,|\Phi_\kappa(a)\rangle$, with a and b characterizing different qp sets. In Eq. (9), $\hat{O}$ stands for $\hat{H}$ or 1.

To calculate $\langle\Phi_{\kappa'}(b)|\,\hat{O}\hat{R}_y(\beta)\,|\Phi_\kappa(a)\rangle$, one must compute the following types of contractions for the Fermion operators

$$\begin{aligned} A_{ij} &= \langle b|\,[\beta]a^\dagger_i a^\dagger_j\,|a\rangle = [V(\beta)U^{-1}(\beta)]_{ij},\\ B_{ij} &= \langle b|\,b_i b_j[\beta]\,|a\rangle = [U^{-1}(\beta)V(\beta)]_{ij},\\ C_{ij} &= \langle b|\,b_i[\beta]a^\dagger_j\,|a\rangle = [U^{-1}(\beta)]_{ij}, \end{aligned} \tag{10}$$

where we have defined

$$[\beta] = \frac{\hat{R}_y(\beta)}{\langle b|\,\hat{R}_y(\beta)\,|a\rangle},$$

and

$$\langle b|\,\hat{R}_y(\beta)\,|a\rangle = [\det U(\beta)]^{1/2}. \tag{11}$$

Equations (10) and (11) are written in a compact form of $N\times N$ matrix, with N being the number of total single particles. The general principle of finding $U(\beta)$ and $V(\beta)$ is given by the Thouless theorem [33], and a well worked-out scheme can be found in the work of Tanabe *et al.* [34] (see also Ref. 35).

To write the matrices $U(\beta)$ and $V(\beta)$ explicitly, we consider the fact that $\{a_i, a^\dagger_i\}$ and $\{b_i, b^\dagger_i\}$ can both be expressed by the spherical representation $\{c_i, c^\dagger_i\}$ through the HFB transformation

$$\begin{aligned} \begin{bmatrix} c\\ c^\dagger \end{bmatrix} &= \begin{pmatrix} U_a & V_a\\ V_a & U_a \end{pmatrix}\begin{bmatrix} a\\ a^\dagger \end{bmatrix}\\ \begin{bmatrix} c\\ c^\dagger \end{bmatrix} &= \begin{pmatrix} U_b & V_b\\ V_b & U_b \end{pmatrix}\begin{bmatrix} b\\ b^\dagger \end{bmatrix}. \end{aligned} \tag{12}$$

U_a, V_a, U_b and V_b in above equations, which define the HFB transformation, are obtained from the Nilsson-BCS calculation. A rotation of the spherical basis can be written in a matrix form as

$$\hat{R}_y(\beta)\begin{bmatrix} c\\ c^\dagger \end{bmatrix}\hat{R}^\dagger_y(\beta) = \begin{pmatrix} d(\beta) & 0\\ 0 & d(\beta) \end{pmatrix}\begin{bmatrix} c\\ c^\dagger \end{bmatrix}. \tag{13}$$

Combining Eqs. (12) and (13) and noting the unitarity of the HFB transformation, one obtains

$$\begin{aligned} \hat{R}_y(\beta)\begin{bmatrix} b\\ b^\dagger \end{bmatrix}\hat{R}^\dagger_y(\beta) = &\begin{pmatrix} U_b & V_b\\ V_b & U_b \end{pmatrix}^T\begin{pmatrix} d(\beta) & 0\\ 0 & d(\beta) \end{pmatrix}\\ &\times\begin{pmatrix} U_a & V_a\\ V_a & U_a \end{pmatrix}\begin{bmatrix} a\\ a^\dagger \end{bmatrix}. \end{aligned} \tag{14}$$

$U(\beta)$ and $V(\beta)$ can finally be obtained from the following equation

$$\begin{aligned} \begin{pmatrix} U(\beta) & V(\beta)\\ V(\beta) & U(\beta) \end{pmatrix} &= \begin{pmatrix} U^T_b & V^T_b\\ V^T_b & U^T_b \end{pmatrix}\begin{pmatrix} d(\beta) & 0\\ 0 & d(\beta) \end{pmatrix}\begin{pmatrix} U_a & V_a\\ V_a & U_a \end{pmatrix}\\ &= \begin{pmatrix} U^T_b d(\beta)U_a + V^T_b d(\beta)V_a & U^T_b d(\beta)V_a + V^T_b d(\beta)U_a\\ V^T_b d(\beta)U_a + U^T_b d(\beta)V_a & U^T_b d(\beta)U_a + V^T_b d(\beta)V_a \end{pmatrix}. \end{aligned}$$

With the overlapping matrix elements that connect configurations belonging to different shapes, one obtains wavefunctions containing configuration mixing. Using these wavefunctions, one can further calculate inter-transition probabilities from a shape isomer to the ground state.

4. Summary

We have introduced the Projected Shell Model description for two kinds of isomers, K-isomers and shape isomers. We have shown that the physics of K-mixing in multi-qp states is well incorporated in the model with the basis states having axial symmetry. Diagonalization mixes configurations of different K, which effectively introduces triaxiality. For K-isomers with much enhanced decay probability to the ground state, a triaxial PSM is needed, which employs γ deformed basis states. On the other hand, projected energy surface calculations have led to a picture of shape coexistence. A scheme has been developed which allows calculations for transition between a shape isomer and the ground state.

The author is grateful to J. Hirsch and V. Velazquez for warm hospitality during the Cocoyoc 2008 meeting. He acknowledges helpful discussions with A. Aprahamian, Y. R.

Shimizu, P. M. Walker, and M. Wiescher. This work is supported by the Chinese Major State Basic Research Development Program through grant 2007CB815005 and by the U. S. National Science Foundation through grant PHY-0216783.

1. P.M. Walker and R.C. Johnson, *Nature Phys.* **3** (2007) 836.
2. I. Mukha *et al.*, *Phys. Rev. Lett.* **95** (2005) 022501.
3. I. Mukha *et al.*, *Nature* **439** (2006) 298.
4. P.M. Walker and G.D. Dracoulis, *Nature* **399** (1999) 35.
5. M. Hasegawa, Y. Sun, K. Kaneko, and T. Mizusaki, *Phys. Lett. B* **617** (2005) 150.
6. E. Bouchez, *et al.*, *Phys. Rev. Lett.* **90** (2003) 082502.
7. A. Blazhev, *et al.*, *Phys. Rev. C* **69** (2004) 064304.
8. Y. Sun, X.-R. Zhou, G.-L. Long, E.-G. Zhao, and P. M. Walker, *Phys. Lett. B* **589** (2004) 83.
9. P.M. Walker and J.J. Carroll, *Physics Today* (June issue) (2005) 39.
10. F.-R. Xu, E.-G. Zhao, R. Wyss, and P.M. Walker, *Phys. Rev. Lett.* **92** (2004) 252501.
11. R.-D. Herzberg *et al.*, *Nature* **442** (2006) 896.
12. A. Aprahamian and Y. Sun, *Nature Phys.* **1** (2005) 81.
13. R.C. Runkle, A.E. Champagne, J. Engel, *Astrophys. J.* **556**, (2001) 970.
14. Y. Sun, M. Wiescher, A. Aprahamian, and J. Fisker, *Nucl. Phys. A* **758** (2005) 765.
15. K. Hara and Y. Sun, *Int. J. Mod. Phys. E* **4** (1995) 637.
16. Y. Sun and K. Hara, *Comp. Phys. Commun.* **104** (1997) 245.
17. K. Jain *et al.*, *Nucl. Phys. A* **591** (1995) 61.
18. V.G. Soloviev, *Nucl. Phys. A* **633** (1998) 247.
19. J.-Y. Zeng, S.-X. Liu, L.-X. Gong, and H.-B. Zhu, *Phys. Rev. C* **65** (2002) 044307.
20. M. Dufour and A.P. Zuker, *Phys. Rev. C* **54** (1996) 1641.
21. S.M. Mullins *et al.*, *Phys. Lett. B* **393** (1997) 279; *Phys. Lett. B* **400** (1997) 401.
22. Y. Sun and J.L. Egido, *Nucl. Phys. A* **580** (1994) 1.
23. G.D. Dracoulis *et al.*, *Phys. Rev. C* **71** (2005) 044326.
24. G.D. Dracoulis *et al.*, *Phys. Lett. B* **635** (2006) 200.
25. C.S. Purry *et al.*, *Nucl. Phys. A* **632** (1998) 229.
26. K. Narimatsu, Y.R. Shimizu, and T. Shizuma, *Nucl. Phys. A* **601** (1996) 69.
27. Y. Sun *et al.*, *Phys. Rev. C* **61** (2000) 064323.
28. Z.-C. Gao, Y.-S. Chen, and Y. Sun, *Phys. Lett. B* **634** (2006) 195.
29. J.A. Sheihk, G.H. Bhat, Y. Sun, G.B. Vakil, and R. Palit, *Phys. Rev. C*, **77** (2008) 034313.
30. Y. Sun, *Eur. Phys. J. A* **20** (2004) 133.
31. K. Kaneko, M. Hasegawa, and T. Mizusaki, *Phys. Rev. C* **70**, (2004) 051301(R).
32. H. Schatz *et. al.*, *Phys. Rep.* **294** (1998) 167.
33. D.J. Thouless, *Nucl. Phys.* **21** (1960) 225.
34. K. Tanabe, K. Enami, and N. Yoshinaga, *Phys. Rev.* **C 59** (1999) 2492.
35. Z.-C. Gao, Y. Sun, and Y.-S. Chen, *Phys. Rev. C.* **74** (2006) 054303.